

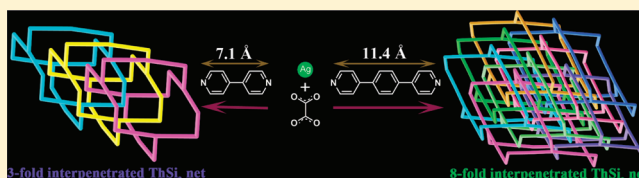
Three- and Eight-Fold Interpenetrated ThSi₂ Metal–Organic Frameworks Fine-Tuned by the Length of Ligand

Di Sun,* Zhi-Hao Yan, Meijiao Liu, Hanyi Xie, Shuai Yuan, Haifeng Lu, Shengyu Feng, and Daofeng Sun*

Key Lab of Colloid and Interface Chemistry, Ministry of Education, School of Chemistry and Chemical Engineering, Shandong University, Jinan, Shandong, 250100, China

Supporting Information

ABSTRACT: Two new interpenetrated ThSi₂ networks, $\{[\text{Ag}_4(\text{bipy})_4(\text{ox})]\cdot 2\text{OH}\cdot 16\text{H}_2\text{O}\}_n$ (**1**) and $\{[\text{Ag}_2(\text{dpb})_2(\text{ox})]\cdot 10\text{H}_2\text{O}\}_n$ (**2**) (bipy = 4,4'-bipyridine, dpb = 1,4-di(pyridin-4-yl)benzene and Na₂ox = sodium oxalate), were constructed from bidentate pyridyl-based organic tectons incorporating ox auxiliary ligand. Interestingly, both **1** and **2** are 3D frameworks with the same ThSi₂ topology but with substantial changes in the interpenetration degrees, which are well controlled by employing the pyridyl-based ligands with different lengths. The thermal stabilities and photoluminescence behaviors of them were also discussed.



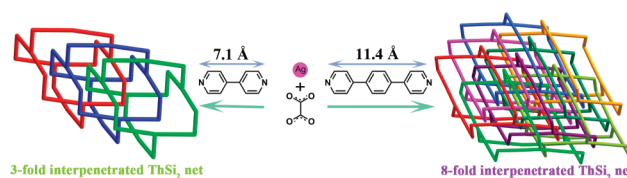
INTRODUCTION

Current interest in polymeric coordination networks, or metal–organic frameworks (MOFs) composed of inorganic and organic building units is rapidly expanding for their intriguing topologies and potential applications in selective molecular recognition and separation, physical gas storage, chemical absorption, luminescence, molecular magnet, ion-exchange, heterogeneous catalysis, and so on.¹ Among the family of MOFs, interpenetration phenomenon has been widely investigated,² and more superiorities of the interpenetrating network have been revealed.³ The origin of interpenetration can be ascribed to the presence of large free spaces in a single network, such as a series of pillared frameworks⁴ and IRMOFs.⁵ Although the investigation on interpenetrated networks advanced rapidly, predicting and control of interpenetration remains a long-standing challenge. As we know, controlling the interpenetrated form and its noninterpenetrated counterpart by modulating the synthetic conditions,⁶ liquid phase epitaxy,⁷ using a well designed organic building block⁸ and sophisticated rod-shaped SBUs,⁹ has been gradually recognized. Recently, an elegant example is temperature and concentration control over interpenetrated and noninterpenetrated primitive cubic (pcu) networks in two isomeric Cd(II) mixed-ligand MOFs reported by the Zaworotko and co-workers.⁶ Very recently, using the solvent molecule as a template to control the degree of interpenetration of pcu network from 2-fold to 3-fold has been reported by Kitagawa group.¹⁰ However, accurately controlling the interpenetration degree of the same topology by length of organic tecton is still in their infancy, even though many interpenetrated frameworks have been widely reported.

We are interested in constructing MOFs with novel topologies and interesting properties from multidentate ligands.¹¹ Recently, by employment of an organic ligand with large steric-hindrance groups, we successfully controlled interpenetration in lanthanide-organic frameworks.¹² As our

continuous work, we attempted to synthesize d¹⁰ transitional metal MOFs and adopted the tecton elongation methodology to fine-tune the interpenetrated degree of the resulting MOFs. Herein, we present an unprecedented example of control over the degree of the interpenetrated frameworks by the length of organic tectons (Scheme 1) in which 3-fold interpenetrated,

Scheme 1. Modulation of Degree of Interpenetration Using Tecton-Elongation Strategy



$\{[\text{Ag}_4(\text{bipy})_4(\text{ox})]\cdot 2\text{OH}\cdot 16\text{H}_2\text{O}\}_n$ (**1**) and 8-fold interpenetrated $\{[\text{Ag}_2(\text{dpb})_2(\text{ox})]\cdot 10\text{H}_2\text{O}\}_n$ (**2**) (bipy = 4,4'-bipyridine, dpb = 1,4-di(pyridin-4-yl)benzene and H₂ox = oxalic acid) with the same ThSi₂ topology were achieved.

EXPERIMENTAL SECTION

Materials and General Methods. Chemicals and solvents used in the syntheses were of analytical grade and used without further purification. 1,4-Di(pyridin-4-yl)benzene ligand was prepared by Pd(PPh₃)₄ catalyzed Suzuki coupling reaction between arylboronic ester and 1,4-dibromobenzene under anaerobic condition. IR spectra were measured on a Nicolet 330 FTIR Spectrometer at the range of 4000–400 cm⁻¹. Elemental analyses were carried out on a CE instruments EA 1110 elemental analyzer. Photoluminescence spectra were measured on a Hitachi F-7000 Fluorescence Spectrophotometer

Received: January 18, 2012

Revised: March 26, 2012

Published: April 12, 2012

(slit width: 5 nm; sensitivity: high). X-ray powder diffractions were measured on a Panalytical X-Pert pro diffractometer with Cu-K α radiation. Thermogravimetric analyses were performed on a NETZSCH TG 209 F1 Iris Thermogravimetric Analyzer from 30 to 800 °C at a heating rate 10 °C/min under the N₂ atmosphere (20 mL/min).

Preparation of Complexes 1 and 2. $\{[Ag_4(bipy)_4(ox)] \cdot 2OH \cdot 16H_2O\}_n$ (**1**). A mixture of Ag₂O (167 mg, 0.5 mmol), bipy·2H₂O (194 mg, 1 mmol) and Na₂ox (134 mg, 1 mmol) was treated in CH₃CH₂OH-H₂O mixed solvent (15 mL, v/v: 1/2) under ultrasonic irradiation at ambient temperature. Then aqueous NH₃ solution (25%) was dropped into the mixture to give a clear solution. The resultant solution was allowed to evaporate slowly in darkness at ambient temperature for several days to give pale-yellow crystals of **1** (yield: 82%, based on Ag). They were washed with a small volume of cold CH₃OH and diethyl ether. Anal. Calcd for C₂₁H₃₃Ag₂N₄O₁₁: C 34.40, H 4.54, N 7.64%. Found: C 34.22, H 4.12, N 7.31%. Selected IR peaks (cm⁻¹): 3418 (s), 3042 (w), 2925 (w), 2852 (w), 1599 (s), 1410 (m), 1385 (s), 1312 (s), 1217 (m), 1070 (w), 990 (w), 803 (m), 617 (w), 506 (w).

$\{[Ag_2(dpb)_2(ox)] \cdot 10H_2O\}_n$ (**2**). Synthesis of **2** was similar to that of **1** but using dpb (232 mg, 1 mmol) instead of bipy·2H₂O in CH₃CH₂OH-H₂O mixed solvent (15 mL, v/v: 4/1). Pale-yellow crystals of **2** were obtained in 76% yield based on Ag Elemental analysis: Anal. Calcd For C₁₈H₃₂Ag₂N₄O₁₄: C 29.05, H 4.33, N 7.52%. Found: C 28.79, H 4.51, N 7.23%. Selected IR peaks (cm⁻¹): 3429 (s), 3123 (w), 2928 (w), 2867 (w), 1571 (s), 1425 (s), 1385 (s), 1302 (w), 1241 (w), 1095 (m), 997 (w), 936 (w), 667 (m).

X-ray Crystallography. Single crystals of the complexes **1** and **2** with appropriate dimensions were chosen under an optical microscope and quickly coated with high vacuum grease (Dow Corning Corporation) before being mounted on a glass fiber for data collection. Data for them were collected on a Bruker Apex II CCD diffractometer with graphite-monochromated Mo K α radiation source ($\lambda = 0.71073$ Å). A preliminary orientation matrix and unit cell parameters were determined from 3 runs of 12 frames each, each frame corresponds to a 0.5° scan in 5 s, followed by spot integration and least-squares refinement. For **1** and **2**, data were measured using ω scans of 0.5° per frame for 10 s until a complete hemisphere had been collected. Cell parameters were retrieved using SMART software and refined with SAINT on all observed reflections.¹³ Data reduction was performed with the SAINT software and corrected for Lorentz and polarization effects. Absorption corrections were applied with the program SADABS.¹³ In all cases, the highest possible space group was chosen. All structures were solved by direct methods using SHELXS-97¹⁴ and refined on F² by full-matrix least-squares procedures with SHELXL-97.¹⁵ Atoms were located from iterative examination of difference F-maps following least-squares refinements of the earlier models. Hydrogen atoms were placed in calculated positions and included as riding atoms with isotropic displacement parameters 1.2–1.5 times U_{eq} of the attached C atoms. All structures were examined using the Addsym subroutine of PLATON¹⁶ to ensure that no additional symmetry could be applied to the models. There are large solvent accessible void volumes in the crystals of both **1** and **2** which are occupied by highly disordered anions and water molecules. No satisfactory disorder model could be achieved, and therefore the SQUEEZE program implemented in PLATON was used to remove these electron densities. Pertinent crystallographic data collection and refinement parameters are collated in Table 1. Selected bond lengths and angles are collated in Table 2.

RESULTS AND DISCUSSION

Synthesis and General Characterization. The growth of single crystals of **1** and **2** was carried out in the darkness to avoid photodecomposition. As is well-known, the reactions of Ag(I) with carboxylates in aqueous solution often result in the formation of microcrystalline or amorphous insoluble silver salts, presumably due to the fast coordination of the carboxylates to Ag(I) ions to form polymers.¹⁷ Hence, properly

Table 1. Crystal Data for 1 and 2

complex	1	2
formula	C ₂₁ H ₃₃ Ag ₂ N ₄ O ₁₁	C ₁₈ H ₃₂ Ag ₂ N ₄ O ₁₄
M _r	733.24	744.20
cryst syst	orthorhombic	orthorhombic
space group	Fddd	Pcca
a (Å)	12.580(2)	26.397(2)
b (Å)	24.563(5)	8.3246(7)
c (Å)	33.566(7)	18.7008(15)
V (Å ³)	10372(3)	4109.4(6)
T (K)	298(2)	298(2)
Z, D _{calcd} (g/cm ³)	16, 1.466	8, 1.242
F(000)	4480	1528
μ (mm ⁻¹)	1.530	0.986
reflns collected/unique	11 236/2286	19 254/3626
R _{int}	0.0755	0.0393
params	132	235
final R indices [I > 2 σ (I)]	R ₁ = 0.0566 ^a wR ₂ = 0.1545 ^b	R ₁ = 0.0318 ^a wR ₂ = 0.0828 ^b
R indices (all data)	R ₁ = 0.0631 ^a wR ₂ = 0.1638 ^b	R ₁ = 0.0415 ^a wR ₂ = 0.0866 ^b
GOF on F ²	1.093	1.037

$${}^a R_1 = \sum |F_o| - |F_c| / \sum |F_o|, \quad {}^b wR_2 = [\sum w(F_o^2 - F_c^2)^2 / \sum w(F_o^2)^2]^{1/2}$$

Table 2. Selected Bond Lengths (Å) and Angles (°) for 1 and 2^a

Complex 1			
Ag1—N2 ⁱ	2.118 (4)	Ag1—O1	2.500 (5)
Ag1—N1	2.131 (4)		
N2 ⁱ —Ag1—N1	166.43 (18)	N1—Ag1—O1	95.52 (17)
N2 ⁱ —Ag1—O1	97.05 (18)		
Complex 2			
Ag1—N1	2.160 (2)	Ag1—O2	2.727 (2)
Ag1—N2 ⁱ	2.161 (2)		
N1—Ag1—N2 ⁱ	163.24 (9)	N2 ⁱ —Ag1—O2	102.23 (8)
N1—Ag1—O1	98.06 (8)	O1—Ag1—O2	47.85 (7)

^aSymmetry codes: (i) $x - 3/4, y + 1/4, -z + 1$; (ii) $-x + 5/4, -y + 5/4, z$; (iii) $-x + 5/4, y, -z + 5/4$. Symmetry codes: (i) $x + 1/2, y + 1, -z$; (ii) $-x + 1, y, -z + 1/2$.

lowering the reaction speed, such as using ammoniacal conditions to form $[Ag(NH_3)_2]^+$ species may favor to the formation of crystalline products.¹⁸ Ag₂O was used instead of AgNO₃ or other common Ag(I) salts to promote the carboxylates instead of small anions to coordinate to the Ag(I) centers. Ultrasonic method has found an important niche in the preparation of inorganic materials.¹⁹ The high local temperatures and pressures, combined with extraordinarily rapid cooling, provide a unique means for driving chemical reactions under extreme conditions. In this system, ultrasound technique also realizes the rapid (10 min) and efficient (max. Thirty different experiments in one batch) preparation of CCs.

Powder X-ray diffraction (PXRD) has been used to check the phase purity of the bulk samples in the solid state. For complexes **1** and **2**, the measured PXRD patterns closely match the simulated patterns generated from the results of single-crystal diffraction data (Figure S1 of the Supporting Information), indicative of pure products. In the IR spectra (Figure S2 of the Supporting Information) of complexes **1** and **2**, the broad peaks at ca. 3400 cm⁻¹ indicate the presence of water molecules. The IR spectra also show characteristic

absorption bands mainly attributed to the asymmetric (ν_{as} : ca. 1600 cm^{-1}) and symmetric (ν_s : ca. 1385 cm^{-1}) stretching vibrations of the carboxylic groups. No band in the region 1690–1730 cm^{-1} indicates complete deprotonation of the carboxylic groups,²⁰ which is consistent with the result of the X-ray diffraction analysis.

Structure Descriptions. $\{[Ag_4(bipy)_4(ox)] \cdot 2OH \cdot 16H_2O\}_n$ (**1**). X-ray single-crystal diffraction analysis reveals that **1** is a unique 3-fold interpenetrated ThSi₂ network. It crystallizes in the orthorhombic crystal system with space group of *Fddd*. The asymmetric unit contains one Ag(I) ion, one bipy ligand and a quarter of ox dianion, and counteranion OH[−] as well as the lattice water molecules in a severely disordered fashion. Two perpendicular 2-fold axes pass through the C11–C11^{iv} bond and the midpoint of C11–C11^{iv} bond, respectively. As depicted in Figure 1a, the Ag1 is located in a T-shaped geometry,

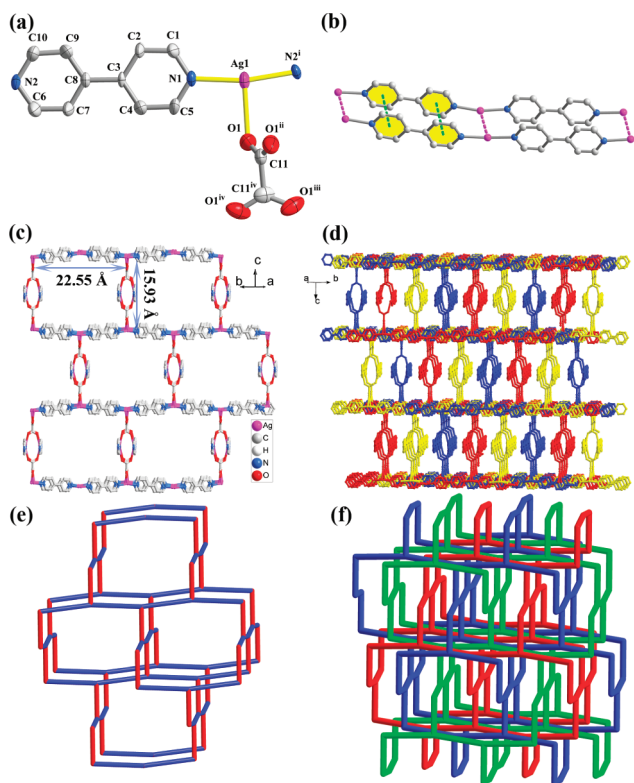


Figure 1. (a) Coordination environment of Ag(I) ion in **1** with the thermal ellipsoids at 50% probability level. (b) Presentation of 1D double-chain incorporating π – π and argentophilic interactions. (c) Ball-and-stick view of single 3D network. (d) 3-fold interpenetrated 3D network. (e) Simplified single ThSi₂ network (red pillar: ox, blue stick: bipy). (f) View of simplified 3-fold interpenetrated ThSi₂ network. (Symmetry codes: (i) $x - 3/4, y + 1/4, -z + 1$, (ii) $-x + 5/4, -y + 5/4, z$; (iii) $-x + 5/4, y, -z + 5/4$ (iv) $-x, -y + 5/4, -z + 5/4$).

completed by two N atoms belonging to two different bipy ligands and one O atoms of ox ligand (Ag1–N1 = 2.131(4), Ag1–N2ⁱ = 2.118(4), and Ag1–O1 = 2.500(5) Å). Both Ag–N and Ag–O bond lengths are well-matched to those observed in similar complexes.²¹ The pyridyl rings of bipy ligand are approximately coplanar with a very small dihedral angle of 3.4°. (Symmetry codes: (i) $x - 3/4, y + 1/4, -z + 1$, (iv) $-x, -y + 5/4, -z + 5/4$).

The Ag(I) ions are bridged by bipy ligands to form a 1D infinite polymeric chain structure, which is generated a double-

chain structure by Agⁱ–Agⁱⁱ interaction. The shortest Ag1ⁱ–Ag1ⁱⁱ separation of 3.2009(10) Å in **1** is comparable to that (3.2146(5) Å) found in previously reported $[Ag_2(bipy)_2(adip) \cdot 6H_2O]_n$ (H₂adip = adipic acid)²² indicating the argentophilic interactions.²³ The double-chains rotate by 78.4° about the normal axis on passing from one sheet to the adjacent one and then turn back to the previous direction on further passing to the successive layer (in a ABAB sequence). Two kinds of face-to-face π – π interactions not only reinforce the 1D double-chains (Cg1ⁱ–Cg2^v = 3.565(4) Å, Figure 1b) but also extend the 1D double-chains to the 2D sheets (Cg1ⁱ–Cg2^{vi} = 3.723(4) Å, Cg1 and Cg2 are the centroids of aromatic ring N1/C1–C5 and N2/C6–C10), which are further joined by μ_4 - η^1 : η^1 : η^1 : η^1 ox ligands along the axis normal to the sheets to form the resulting cationic 3D framework (Figure 1c and d). (Symmetry codes: (ii) $-x + 5/4, -y + 5/4, z$; (v) $-x + 2, -y + 1, -z + 1$; (vi) $-x + 9/4, -y + 5/4, z$).

The topological analysis of **1** by TOPOS software²⁴ reveals that the 3D network of **1** belongs to a ThSi₂ network (part e of Figure 1) with the vertex symbol of $\{10_2 \cdot 10_4 \cdot 10_4\}$. If the Ag(I) ions are considered as 3-connected nodes, bipy and ox ligands are both considered as the same kind of linkers, then, each node has three angles and each of the angles forms part of a 10-membered shortest circuit and hence the 3D network has the Wells point symbol/Schläfli symbol of 10^3 .²⁵ To explain the vertex symbol further, in the ThSi₂ network one angle is associated with two 10-membered fundamental rings and the other two angles are associated with four 10-membered fundamental rings. The single 3D network consists of large rectangular windows with the size of 22.55 × 15.93 Å, which are filled via mutual interpenetration of three independent equivalent networks, generating a 3-fold interpenetrated 3D network (Figure 1f). An analysis of the interpenetration according to a recent classification²⁶ reveals that **1** belongs to Class Ia (all the interpenetrated nets are generated only by translation and the translating vector is crystallographic *a* axis (12.580(2) Å). Despite the 3-fold interpenetrated 3D network, complex **1** still shows an unusual open framework containing solvent-accessible voids. Guest OH[−] anions and lattice water molecules reside in the voids. The PLATON¹⁶ reveals that the voids in complex **1** occupy 35.0% of the crystal volume (after the removal of the guest molecules and anions).

$\{[Ag_2(dpb)_2(ox)] \cdot 10H_2O\}_n$ (**2**). When using longer pyridyl-based organic tecton, we obtained complex **2** as a 8-fold interpenetrated ThSi₂ network. Complex **2** crystallizes in the orthorhombic crystal system with space group of *Pcca*. The asymmetric unit of **2** contains one Ag(I) ion, one dpb ligand, a half of ox dianion, and the lattice water molecules in a severely disordered fashion. One 2-fold axis passes through the midpoint of C17–C17ⁱⁱ bond. As shown in Figure a, the Ag1 is located in a T-shaped geometry, completed by two N atoms belonging to two different dpb ligands and one O atoms of ox ligand (Ag1–N1 = 2.160(2), Ag1–N2ⁱ = 2.161(2), and Ag1–O1 = 2.702(3) Å). The central phenyl ring is noncoplanar with respect to two terminal pyridyl rings giving two dihedral angles of 16.4 and 16.2°, respectively. (Symmetry codes: (i) $x + 1/2, y + 1, -z$; (ii) $-x + 1, y, -z + 1/2$).

The Ag(I) ions are bridged by dpb ligands to form a 1D infinite polymeric chain structure without Agⁱ–Agⁱⁱ interaction. The adjacent single chains rotate by 74.8° about the normal axis. The π – π interactions (3.749 (4) and 3.813(4) Å) extend the 1D single chains to the 2D sheets which are further joined

by the $\mu_2\text{-}\eta^1\text{:}\eta^0\text{:}\eta^1\text{:}\eta^0$ ox ligands along the axis normal to the sheets to form the resulting neutral 3D framework.

Interestingly, TOPOS analysis of the 3D framework of **2** gives the same topology to that of **1** but with different interpenetration degree and type. The single 3D network of **2** consists of much larger rectangular windows compared to that in **1** with the dimension of $31.21 \times 16.94 \text{ \AA}$ (Figure 2a and b).

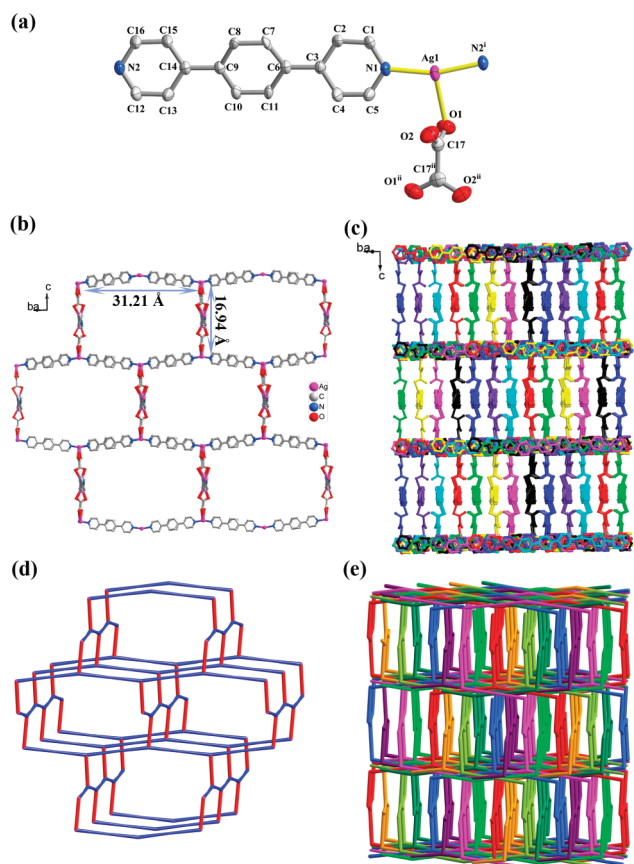
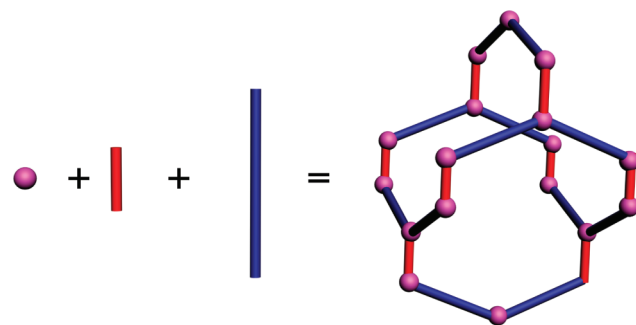


Figure 2. (a) Coordination environment of Ag(I) ion in **2** with the thermal ellipsoids at 50% probability level. (b) Ball-and-stick view of single 3D network. (c) 8-fold interpenetrated 3D network. (d) Simplified single ThSi₂ network (red pillar: ox, blue stick: dpb). (e) View of simplified 8-fold interpenetrated ThSi₂ network.

As a consequence of Mother Nature's horror vacui, complex **2** adopts 8-fold interpenetration to avoid extremely large voids (Figure 2c and e). However, in spite of interpenetration, **2** still possesses free void space estimated to be about 1423.0 \AA^3 , that is, 34.6% of the unit cell. The disordered water molecules occupied the free void. Interestingly, complex **2** belongs to rare Class IIIa interpenetration, that is, the overall interpenetration is generated both by pure translations and by space group symmetry elements. In details, the translationally related four ThSi₂ nets are observed showing the only one translational interpenetrating vector of [010] (also known as crystallographic *b* axis), then, the presence of a nontranslational interpenetrating symmetry element (inversion center) generates the overall 8-fold interpenetration, which is completely different from the Class Ia interpenetration observed in **1**. As we know, the 2-, 3-, 4-, 6-, and highest 9-fold interpenetrated ThSi₂ nets have been documented in the literatures,²⁷ however, 8-fold interpenetrated ThSi₂ net, especially Class IIIa interpenetrated ThSi₂ net, has not been observed yet.

Effect of the Tecton Length on the Interpenetration Degree. Complexes **1** and **2** are 3D networks with ThSi₂ topology but with different interpenetration degree based on Ag(I) 3-connected node linked by mixed rodlike tectons, bipy or dpb and ox. The structural analysis indicates that the length of tecton has little effect on the formation of the ThSi₂-type MOFs, but can obviously adjust the degree of interpenetration of MOFs. To the best of our knowledge, interpenetration can be sensitively affected by interactions between the neighboring networks, steric-hindrance group, chemical functionality and van der Waals surface areas of the organic tectons.²⁸ However, this has not yet been elucidated to date, although several strategies have been shown to influence interpenetration.²⁹ Surprisingly and fortunately, the tecton elongation show negligible influence on the main structures in this system, which facilitates us to investigate the correlation of degree of interpenetration with length of tecton. In **1** and **2**, auxiliary ox ligand has a fixed length and Ag(I) ion keeps its nature of 3-connected node, but bipy and dpb tectons have obviously different lengths of 7.1 and 11.4 Å, respectively (Scheme 2), as

Scheme 2. Schematic Representation of the Assembly of Metal Ions and Mixed Organic Tectons (Purple Ball: Ag(I) Ion, Red Rod: ox, Blue Rod: bipy or dpb) to Yield ThSi₂ Topology



a consequence, similar 3D networks with the identical 3-connected ThSi₂ topology but incorporating different size of void space were obtained. The larger void space can accommodate much more equivalent networks resulting higher degree of interpenetration. Although **1** and **2** contain singly- and doubly stranded chains respectively, the topology of network and degree of interpenetration, at least in this system, are not sensitive to the kind of chain. To prove this viewpoint, we introduced our previously reported complex **3** ($[\text{Ag}_2(\text{bipy})_2(\text{ox}) \cdot 7\text{H}_2\text{O}]_n$)²² into this work. This complex is also a 3-fold interpenetrated ThSi₂ network similar to **1** but incorporating singly strand chain. By structural comparison of **1**, **2**, and **3** shown in Table 3, we can conclude that different types of chains have little effect on the resultant interpenetrated networks, which are mainly controlled by the length of the ligand. At present, although the influences of the tecton length on interpenetration degree are only observed in two closely

Table 3. Structural Comparison of **1**, **2**, and **3**

complex	1 (this work)	2 (this work)	3 (ref 22)
type of chain	doubly stranded	singly stranded	singly stranded
N-donor (length/Å)	bipy (7.1)	dpb (11.4)	bipy (7.1)
O-donor	ox	ox	ox
interpenetration	3-fold ThSi ₂	8-fold ThSi ₂	3-fold ThSi ₂

related examples, the results described herein provide an indication that simple but efficient ways to control interpenetration degree of the same topology in MOFs are at hand.

Thermal Analysis. The thermogravimetric (TG) measurements were performed in N₂ atmosphere on polycrystalline samples of complexes **1** and **2** and the TG curves are shown in Figure S3 of the Supporting Information. The TGA curve of **1** displays a weight loss of 21.02% (Calcd 19.66%) at 30–146 °C corresponds to complete loss of lattice water molecules. Then, the framework starts to collapse. Complex **2** shows a first weight loss of 11.67% at 30–118 °C corresponding to the loss of lattice water molecule (Calcd 12.10%). The dehydrated framework is stable to 180 °C and then the framework begins to collapse accompanying the release of organic ligands.

Photoluminescence Properties. Recently, inorganic–organic hybrid complexes, especially comprising the d¹⁰ closed-shell metal center and aromatic-containing system, have been intensively investigated for attractive fluorescence properties and potential applications, such as chemical sensors, white light-emitting diodes (LEDs), and electroluminescent materials (OLEDs) for displays.³⁰ Figure 3 shows the

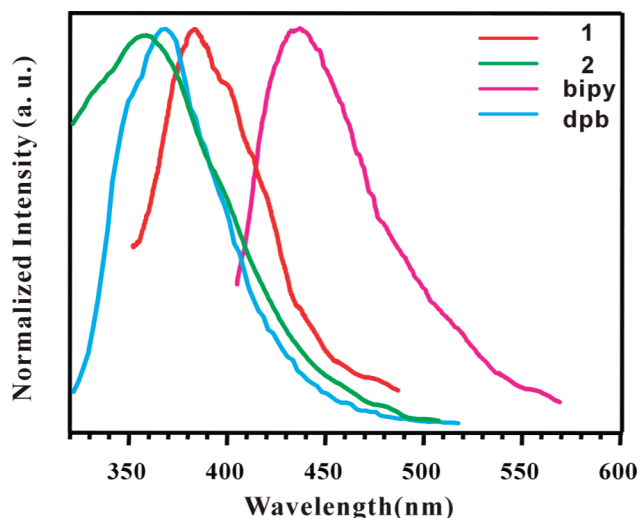


Figure 3. Photoluminescences of free ligands and complexes **1** and **2**.

photoluminescence spectra of the free ligands and complexes **1** and **2**. The free ligands bipy and dpb display photoluminescence with emission maxima at 436 and 367 nm ($\lambda_{\text{ex}} = 300$ nm), respectively. It can be presumed that these peaks originate from the $\pi^* \rightarrow n$ or $\pi^* \rightarrow \pi$ transitions. Upon complexation of these ligands with Ag(I) ion, intense emissions are observed at 385 nm ($\lambda_{\text{ex}} = 330$ nm) for **1** and 358 nm ($\lambda_{\text{ex}} = 330$ nm) for **2**, respectively. The resemblance between the emissions of **1** and **2** and those of the free bipy and dpb indicates that the emissions of **1** and **2** are probably attribute to the intraligand (IL) $\pi \rightarrow \pi^*$ transitions modified by metal coordination.³¹ In comparison with **1**, a blue shift of 27 nm has been observed in **2** which are probably attributable to the differences of ligands and the absence of Ag...Ag interaction in **1**.³² These observation indicates that both **1** and **2** may be excellent candidate for potential photoluminescent materials.

CONCLUSIONS

In conclusion, two new MOFs based on 3-connected Ag(I) node with two structurally related rodlike pyridyl-based tectons

incorporating auxiliary oxalate, have been synthesized and characterized and provide new examples of interpenetrated systems. The tecton elongation strategy was successfully used to fine-tune the degree of interpenetration. Two ThSi₂ networks with different degrees of interpenetration, 3-fold for **1** and 8-fold for **2**, were obtained simply and cleanly by modulating the length of pyridyl-based organic tectons, that is, longer tecton favored the higher interpenetration degree and vice versa. The extension of this strategy to other tectons and metal centers is currently under investigation.

ASSOCIATED CONTENT

Supporting Information

Crystallographic data in CIF format, powder X-ray diffraction (PXRD) patterns, TGA and IR spectra for **1** and **2**, ¹H NMR and ESI-MS for 1,4-di(pyridin-4-yl)benzene ligand. CCDC 864082 (**1**) and 864083 (**2**). This material is available free of charge via the Internet at <http://pubs.acs.org>.

AUTHOR INFORMATION

Corresponding Author

*E-mail: dsun@sdu.edu.cn, dfsun@sdu.edu.cn; Fax: +86-531-88364218.

Notes

The authors declare no competing financial interest.

ACKNOWLEDGMENTS

This work was supported by the NSFC (Grant No. 90922014), the Shandong Natural Science Fund for Distinguished Young Scholars (2010JQE27021), the NSF of Shandong Province (BS2009L007, Y2008B01), Independent Innovation Foundation of Shandong University (2010JQ011 and 2011GN030), and the Special Fund for Postdoctoral Innovation Program of Shandong Province (201101007).

REFERENCES

- (1) (a) Kong, X.-J.; Long, L.-S.; Zheng, Z.; Huang, R.-B.; Zheng, L.-S. *Acc. Chem. Res.* **2010**, *43*, 201. (b) Rusanov, E. B.; Ponomarova, V. V.; Komarchuk, V. V.; Stoeckli-Evans, H.; Fernandez-Ibanez, E.; Stoeckli, F.; Sieler, J.; Domasevitch, K. V. *Angew. Chem., Int. Ed.* **2003**, *42*, 2499. (c) Würthner, F.; You, C.-C.; Saha-Möllner, C. R. *Chem. Soc. Rev.* **2004**, *33*, 133. (d) Chen, B.; Xiang, S.; Qian, G. *Acc. Chem. Res.* **2010**, *43*, 1115. (e) Yoshizawa, M.; Klosterman, J. K.; Fujita, M. *Angew. Chem., Int. Ed.* **2009**, *48*, 3418. (f) Gibb, C. L. D.; Gibb, B. C. *J. Am. Chem. Soc.* **2004**, *126*, 11408. (g) Chen, L.; Jiang, F.; Lin, Z.; Zhou, Y.; Yue, C.; Hong, M. *J. Am. Chem. Soc.* **2005**, *127*, 8588. (h) Su, W.; Hong, M. *Angew. Chem., Int. Ed.* **2000**, *39*, 2911. (i) Yaghi, O. M.; Tranchemontagne, D. J.; Mendoza-Cortes, J. L.; O'Keeffe, M. *Chem. Soc. Rev.* **2009**, *38*, 1257. (j) Yuan, D. Q.; Zhao, D.; Sun, D. F.; Zhou, H. C. *Angew. Chem., Int. Ed.* **2010**, *49*, 5357. (k) Domasevitch, K. V.; Solntsev, P. V.; Gural'skiy, I. A.; Krautscheid, H.; Rusanov, E. B.; Chernega, A. N.; Howard, J. A. K. *Dalton Trans.* **2007**, 3893. (l) Sun, D. F.; Ma, S. Q.; Ke, Y. X.; Collins, D. J.; Zhou, H. C. *J. Am. Chem. Soc.* **2006**, *128*, 3896. (m) Tanabe, K. K.; Allen, C. A.; Cohen, S. M. *Angew. Chem., Int. Ed.* **2010**, *49*, 9730. (n) Su, C.-Y.; Cai, Y.-P.; Chen, C.-L.; Smith, M. D.; Kaim, W.; Zur Loye, H.-C. *J. Am. Chem. Soc.* **2003**, *125*, 8595. (o) Perry, J. J.; Perman, J. A.; Zaworotko, M. J. *Chem. Soc. Rev.* **2009**, *38*, 1400. (p) Moulton, B.; Zaworotko, M. J. *Chem. Rev.* **2001**, *101*, 1629. (2) (a) Batten, S. R.; Robson, R. *Angew. Chem., Int. Ed.* **1998**, *37*, 1460. (b) Chen, W. X.; Wu, S. T.; Long, L. S.; Huang, R. B.; Zheng, L. S. *Cryst. Growth Des.* **2007**, *7*, 1171. (3) (a) Ha, S. M.; Yuan, W.; Pei, Q.; Pelrine, R.; Stanford, S. *Adv. Mater.* **2006**, *18*, 887. (b) Liu, C. M.; Gao, S.; Zhang, D. Q.; Huang, Y. H.; Xiong, R. G. *Angew. Chem., Int. Ed.* **2004**, *43*, 990. (c) Yaghi, O. M.

- Nat. Mater.* **2007**, *6*, 92. (d) Maji, T. K.; Matsuda, R.; Kitagawa, S. *Nat. Mater.* **2007**, *6*, 142. (e) Kitagawa, S.; Kitaura, R.; Noro, S. *Angew. Chem., Int. Ed.* **2004**, *43*, 2334.
- (4) (a) Ma, B. Q.; Mulfort, K. L.; Hupp, J. T. *Inorg. Chem.* **2005**, *44*, 4912. (b) Chen, B. L.; Ma, S. Q.; Zapata, F.; Lobkovsky, E. B.; Yang, J. *Inorg. Chem.* **2006**, *45*, 5718. (c) Chun, H.; Dybtsev, D. N.; Kim, H.; Kim, K. *Chem.—Eur. J.* **2005**, *11*, 3521.
- (5) (a) Eddaoudi, M.; Kim, J.; Rosi, N.; Vodak, D.; Wachter, J.; O’Keeffe, M.; Yaghi, O. M. *Science* **2002**, *295*, 469. (b) Chen, B.; Wang, X. J.; Zhang, Q. F.; Xi, X. Y.; Cai, J. J.; Qi, H.; Shi, S.; Wang, J.; Yuan, D.; Fang, M. *J. Mater. Chem.* **2010**, *20*, 3758.
- (6) Zhang, J. J.; Wojtas, L.; Larsen, R. W.; Eddaoudi, M.; Zaworotko, M. J. *J. Am. Chem. Soc.* **2009**, *131*, 17040.
- (7) Shekhah, O.; Wang, H.; Paradinas, M.; Ocal, C.; Schupbach, B.; Terfort, A.; Zacher, D.; Fischer, R. A.; Woll, C. *Nat. Mater.* **2009**, *8*, 481.
- (8) Farha, O. K.; Malliakas, C. D.; Kanatzidis, M. G.; Hupp, J. T. *J. Am. Chem. Soc.* **2010**, *132*, 950.
- (9) Rosi, N. L.; Kim, J.; Eddaoudi, M.; Chen, B. L.; O’Keeffe, M.; Yaghi, O. M. *J. Am. Chem. Soc.* **2005**, *127*, 1504.
- (10) Bureekaew, S.; Sato, H.; Matsuda, R.; Kubota, Y.; Hirose, R.; Kim, J.; Kato, K.; Takata, M.; Kitagawa, S. *Angew. Chem., Int. Ed.* **2010**, *49*, 7660.
- (11) (a) Sun, J.; Dai, F. N.; Yuan, W. B.; Bi, W. H.; Zhao, X. L.; Sun, W. M.; Sun, D. F. *Angew. Chem., Int. Ed.* **2011**, *50*, 7061. (b) Zhao, X. L.; He, H. Y.; Hu, T. P.; Dai, F. N.; Sun, D. F. *Inorg. Chem.* **2009**, *48*, 8057. (c) Dai, F. N.; Dou, J. M.; He, H. Y.; Zhao, X. L.; Sun, D. F. *Inorg. Chem.* **2010**, *49*, 4117. (d) Dai, F. N.; He, H. Y.; Sun, D. F. *Inorg. Chem.* **2009**, *48*, 4613. (e) Zhao, X. L.; He, H. Y.; Dai, F. N.; Sun, D. F.; Ke, Y. X. *Inorg. Chem.* **2010**, *49*, 8650. (f) Dai, F. N.; He, H. Y.; Sun, D. F. *J. Am. Chem. Soc.* **2008**, *130*, 14064.
- (12) He, H. Y.; Yuan, D. Q.; Ma, H. Q.; Sun, D. F.; Zhang, G. Q.; Zhou, H. C. *Inorg. Chem.* **2010**, *49*, 7605.
- (13) Bruker. SMART, SAINT and SADABS. Bruker AXS Inc., Madison, Wisconsin, USA, 1998.
- (14) Sheldrick, G. M. *SHELXS-97, Program for X-ray Crystal Structure Determination*; University of Gottingen: Germany, 1997.
- (15) Sheldrick, G. M. *SHELXL-97, Program for X-ray Crystal Structure Refinement*; University of Gottingen: Germany, 1997.
- (16) Spek, A. L. *Implemented as the PLATON Procedure, a Multipurpose Crystallographic Tool*; Utrecht University: Utrecht, The Netherlands, 1998.
- (17) Smith, G.; Reddy, A. N.; Byriel, K. A.; Kennard, C. H. L. *J. Chem. Soc., Dalton Trans.* **1995**, 3565.
- (18) (a) Hao, H. Q.; Liu, W. T.; Tan, W.; Lin, Z. J.; Tong, M. L. *Cryst. Growth Des.* **2009**, *9*, 457. (b) Sun, D.; Luo, G. G.; Zhang, N.; Wei, Z. H.; Yang, C. F.; Xu, Q. J.; Huang, R. B.; Zheng, L. S. *Chem. Lett.* **2010**, *39*, 190.
- (19) (a) McNamara, W. B., III; Didenko, Y.; Suslick, K. S. *Nature* **1999**, *401*, 772. (b) Flannigan, D. J.; Suslick, K. S. *Nature* **2005**, *434*, 52.
- (20) Nakamoto, K. *Infrared and Raman Spectra of Inorganic and Coordination Compounds*; John Wiley & Sons: New York, 1986.
- (21) (a) Boldog, I.; Rusanov, E. B.; Sieler, J.; Blaurock, S.; Domasevitch, K. V. *Chem. Commun.* **2003**, 740. (b) Gural’skiy, I. A.; Solntsev, P. V.; Krautscheid, H.; Domasevitch, K. V. *Chem. Commun.* **2006**, 4808. (c) Boldog, I.; Daran, J.-C.; Chernega, A. N.; Rusanov, E. B.; Krautscheid, H.; Domasevitch, K. V. *Cryst. Growth Des.* **2009**, *9*, 2895. (d) Gural’skiy, I. A.; Escudero, D.; Frontera, A.; Solntsev, P. V.; Rusanov, E. B.; Chernega, A. N.; Krautscheid, H.; Domasevitch, K. V. *Dalton Trans.* **2009**, 2856. (e) Domasevitch, K. V.; Solntsev, P. V.; Gural’skiy, I. A.; Krautscheid, H.; Rusanov, E. B.; Chernega, A. N.; Howard, J. A. K. *Dalton Trans.* **2007**, 3893.
- (22) Sun, D.; Xu, H.-R.; Yang, C.-F.; Wei, Z.-H.; Zhang, N.; Huang, R.-B.; Zheng, L.-S. *Cryst. Growth Des.* **2010**, *10*, 4642.
- (23) Pyykkö, P. *Chem. Rev.* **1997**, *97*, 597.
- (24) Blatov, V. A. *IUCr CompComm Newsletter* **2006**, *7*, 4 see also <http://www.topos.ssu.samara.ru>.
- (25) Wells, A. F. *Three-Dimensional Nets and Polyhedra*; Wiley-Interscience: New York, 1977.
- (26) Blatov, V. A.; Carlucci, L.; Ciani, G.; Proserpio, D. M. *CrystEngComm* **2004**, *6*, 377.
- (27) (a) Biradha, K.; Fujita, M. *Angew. Chem., Int. Ed.* **2002**, *41*, 3392. (b) Carlucci, L.; Ciani, G.; Proserpio, D. M.; Sironi, A. *J. Am. Chem. Soc.* **1995**, *117*, 4562. (c) Choe, W.; Kiang, Y.-H.; Xu, Z.; Lee, S. *Chem. Mater.* **1999**, *11*, 1776. (d) Yaghi, O. M.; Li, H. *J. Am. Chem. Soc.* **1995**, *117*, 10401. (e) Wang, H.-Y.; Gao, S.; Huo, L.-H.; Ng, S. W.; Zhao, J.-G. *Cryst. Growth Des.* **2008**, *8*, 665.
- (28) Gadzikwa, T.; Zeng, B.-S.; Hupp, J. T.; Nguyen, S. T. *Chem. Commun.* **2008**, 3672.
- (29) (a) Long, D. L.; Hill, R. J.; Blake, A. J.; Champness, N. R.; Hubberstey, P.; Wilson, C.; Schröder, M. *Chem.—Eur. J.* **2005**, *11*, 1384. (b) Li, Z.-X.; Hu, T.-L.; Ma, H.; Zeng, Y.-F.; Li, C.-J.; Tong, M.-L.; Bu, X.-H. *Cryst. Growth Des.* **2010**, *10*, 1138. (c) Li, Z.-X.; Xu, Y.; Zuo, Y.; Li, L.; Pan, Q.; Hu, T.-L.; Bu, X.-H. *Cryst. Growth Des.* **2009**, *9*, 3904.
- (30) (a) Wu, Q.; Esteghamatian, M.; Hu, N.-X.; Popovic, Z.; Enright, G.; Tao, Y.; D’Iorio, M.; Wang, S. *Chem. Mater.* **2000**, *12*, 79. (b) Chen, Y. D.; Qin, Y. H.; Zhang, L. Y.; Shi, L. X.; Chen, Z. N. *Inorg. Chem.* **2004**, *43*, 1197. (c) Santis, G. D.; Fabbri, L.; Licchelli, M.; Poggi, A.; Taglietti, A. *Angew. Chem., Int. Ed.* **1996**, *35*, 202. (d) Wu, H. B.; Huang, Z. J.; Wang, Q. M. *Chem.—Eur. J.* **2010**, *16*, 12321. (e) Li, G.; Lei, Z.; Wang, Q.-M. *J. Am. Chem. Soc.* **2010**, *132*, 17678. (f) Jia, J.-H.; Wang, Q.-M. *J. Am. Chem. Soc.* **2009**, *131*, 16634.
- (31) Fang, X.-Q.; Deng, Z.-P.; Huo, L.-H.; Wan, W.; Zhu, Z.-B.; Zhao, H.; Gao, S. *Inorg. Chem.* **2011**, *50*, 12562.
- (32) Yam, V. W.-W.; Lo, K. K.-W. *Chem. Soc. Rev.* **1999**, *28*, 323.